

Non-contact equipment fault detection using audio and magnetic sensors

Zhimin Yuan^{1,#}, Wee Tiong Tey¹, Tomasz Karol Maszczyk¹, Daniel Lim¹, Sivakumar Nadarajan²,
Viswanathan Vaiyapuri², Amit Gupta², and Sathyanarayan Rajaram³

¹ Industrial IoT Innovation, A*STAR, #05-06, CleanTech Two, Singapore 637143

² Roll-Royce Electrical, Singapore 637718

³ Roll-Royce @NTU Corporate Lab, Singapore 637718

#Email: yuan_zhimin@i3.a-star.edu.sg, TEL: +65-67149419

KEYWORDS: Machine fault, Non-contact sensing, Audio sensor, Magnetic sensor

The accelerometer is widely used to measure the vibrations of equipment for monitoring the health condition and predicting the potential failure of the equipment. In the application, the accelerometer has to mount on the equipment rigidly for getting the good quality vibration signals. Adding the accelerometer on the existing equipment could be a challenge due to the space limitation, the right location, etc. It is beneficial to have non-contact sensor to monitor equipment condition for the detection of the anomaly and the fault. This paper applies the audio sensor for the vibration monitoring and the magnetic sensor for motor operation monitoring both in non-contact deployment on the equipment fault simulator. The audio sensor is able to detect both bearing fault and gear fault. The magnetic sensor can detect gear fault.

1. Introduction

The equipment health monitoring enables the health visibility of the overall system and detects the components in the system causing the health issue, which helps to fix the problem early and efficiently. Otherwise, it may encounter the potential equipment downtime with increased maintenance cost and even damage the equipment causing the revenue loss. The high-end accelerometers are widely applied to monitor the vibration conditions of the equipment for anomaly and fault detection. Mounting the high cost accelerometers on the existing equipment could be a challenge due to the space limitation, the power availability, the right location, etc. It is beneficial to have non-contact sensors to monitor equipment conditions for both anomaly and fault detection.

This paper uses non-contact audio sensor and magnetic sensor for monitoring the equipment conditions. Both sensors are deployed near the equipment fault simulator with the controlled faulty modes, such as the bearing fault, the gear fault, and compare with the health condition for sensor performance study.

2. Non-contact sensors and result discussions

This study uses a customized equipment fault simulator to create different equipment conditions for the performance evaluation of

non-contact sensors. In the equipment fault simulator, the faulty parts are exchangeable inside the gearbox for the creation of bearing fault and gear fault in comparison to the equipment healthy condition. Due to the tight fit of some mechanical parts, there is a repeatability concern on mechanical features. In the study, there are three iterations of changing parts from healthy to bearing fault, then gear fault, and back to healthy. It is to ensure the selected sensor features are significant and well repeatable.

The tunneling magneto-resistive (TMR) sensor measures magnetic signals from the motor in the equipment fault simulator. Comparing to conventional Hall sensor, the TMR sensor has over 100 times SNR gain with good signal quality. The TMR sensor need to be located near the motor without the necessity of the contact to the motor. In the sensor deployment, it usually moves the TMR sensor around to search a location with more magnetic flux leakage from the running motor for picking up stronger magnetic signals.

The MEMS audio sensors are massive produced for mobile phone application. The MEMS audio sensor usually has a bandwidth of 20 KHz, which is wide enough for all the frequency modes of vibrations. One challenge of applying audio sensor is the pickup of background noise. At the noisy environment, the noise floor is easily 30dB to 40dB higher than the quiet lab. Then, some of the weaker vibration signals become not detectable. Usually the MEMS audio sensor is 180° directional with zero noise pickup from the backside. The tuning

of audio sensor facing is able to reduce the noise floor effectively.

2.1 Result analysis of magnetic sensor

Fig.1 shows the raw signal from TMR sensor when the motor runs at 2040 RPM. There are 3-pole pairs in the motor. The magnetic moment of each pole pair varies but the signals are well repeatable. The peak amplitude variations of the fundamental harmonic as motor running at 2040 RPM over three iterations of healthy, bearing fault and gear fault are within 0.25dB.

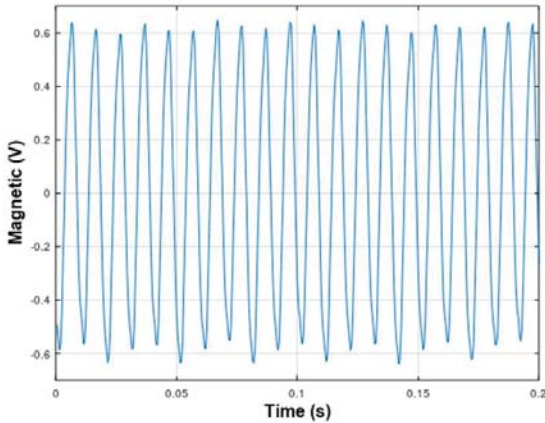


Fig. 1 The raw signal of magnetic sensor from the motor running at 2040 RPM.

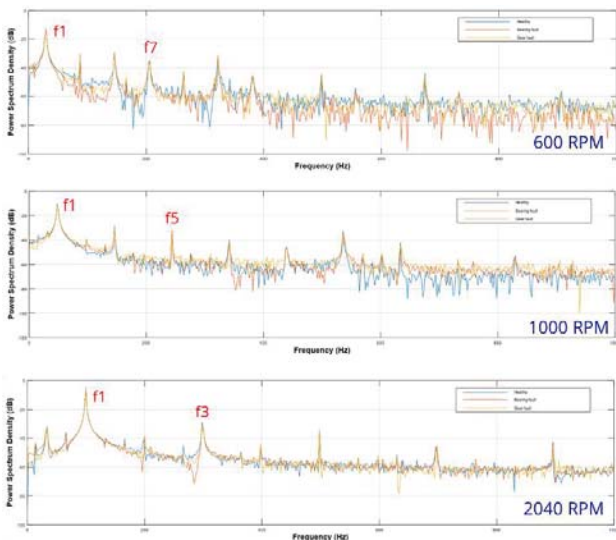


Fig. 2 The power spectrum density of magnetic signals at 600 RPM, 1000 RPM, and 2040 RPM

The power spectrum density (PSD) of magnetic signal is plotted in Fig. 2 at 600 RPM, 1000 RPM, and 2040 RPM, respectively. At each motor speed, the spectrums of healthy condition, bearing fault, and gear fault are compared together. There are substantial PSD variations near the baseline or the noise floor. The PSD variation near the baseline is also big for the same condition among three different iterations. Consider the good repeatability of fundamental harmonic signal, which is 20 dB higher than the rest odd harmonics, such PSD variation near the baseline is most likely related to the parts changing at gearbox.

In order to minimize the impact of the repeatability from the parts changing at gearbox, we focus on the feature of harmonic signals over different iterations. Table 1 lists the selected harmonic signals to determine the gear fault at different motor speed. At 600 RPM, the 7th harmonic of magnetic signal can differentiate the gear fault from the healthy condition for all the 3 iterations. Use the fundamental harmonic signal as a reference, the 7th harmonic of gear fault is above 1dB lower than that of healthy condition. The gear fault has lower signal intensity for the 5th harmonic at 1000 RPM and the 3rd harmonic at 2040 RPM. The magnetic sensor is able to detect gear fault at different motor speed. In general, the signal intensity of bearing fault tends to be lower than the healthy condition at above harmonics of respective motor speed. But there is the outlier at one of the iterations. The confidence level is lower to detect bearing fault using magnetic sensor.

Table 1 The selected harmonics of magnetic signal to determine the gear fault of the equipment fault simulator

Iteration	Signal intensity (dB) @ 600 RPM			
	Healthy		Gear fault	
	f1	f7	f1	f7
1	-12.953	-34.697	-13.03	-36.003
2	-12.674	-34.595	-12.796	-35.581
3	-13.541	-34.864	-12.993	-35.561

Iteration	Signal intensity (dB) @ 1000 RPM			
	Healthy		Gear fault	
	f1	f5	f1	f5
1	-11.345	-31.876	-11.57	-33.686
2	-10.569	-31.855	-11.259	-33.752
3	-11.363	-33.068	-11.405	-33.572

Iteration	Signal intensity (dB) @ 2040 RPM			
	Healthy		Gear fault	
	f1	f3	f1	f3
1	-4.8659	-29.6963	-4.8761	-30.3997
2	-4.6717	-29.096	-4.8068	-30.8776
3	-4.9195	-29.9126	-4.753	-30.9813

2.2 Result analysis of audio sensor

Fig. 3 shows the power spectrum density of audio sensor at 600 RPM, 1000 RPM, and 2040 RPM, respectively. The detected major vibration modes are changing at different motor speeds. The reason could be the motor running at different speed excites different parts to vibrate more. At each motor speed, one of the major vibration modes is selected to detect the conditions of equipment fault simulator.

At 600 RPM, the signal intensity at 248 Hz vibration mode is measured for all the three conditions over three iterations. As shown in Table 2, both bearing fault and gear fault induce higher intensity of vibrations than the healthy condition. It is noticed that the gear fault

of the 3rd iteration at 600 RPM is marginal higher than the healthy condition. At 1000 RPM, both bearing fault and gear fault have higher vibration intensity than the healthy condition at the vibration mode of 310 Hz., where the gear fault has larger vibration intensity over all 3 iterations. At 2040 RPM, both bearing fault and gear fault have higher vibration intensity at vibration mode of 210 Hz, where the bearing fault induces higher intensity of vibrations.

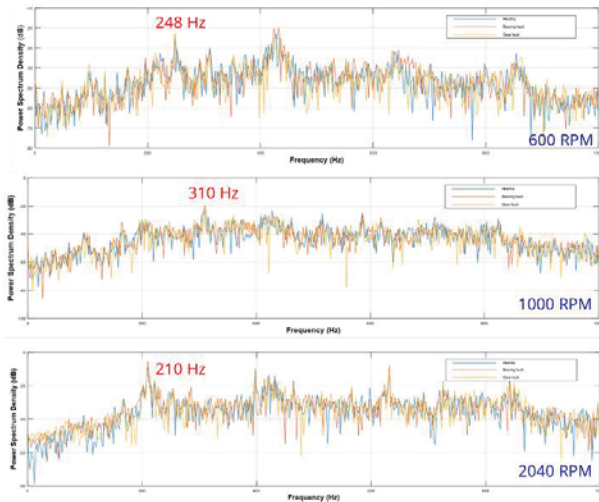


Fig. 3 The power spectrum density of audio signals at 600 RPM, 1000 RPM, and 2040 RPM.

Table 2 The signal intensity of different equipment conditions at 248 Hz for 600 RPM, 310 Hz for 1000 RPM, and 210 Hz for 2040 RPM

Signal intensity (dB) @ 600 RPM			
Iteration	Healthy	Bearing	Gear
1	-27.627	-25.284	-24.178
2	-24.498	-22.796	-23.422
3	-27.245	-25.446	-27.071

Signal intensity (dB) @ 1000 RPM			
Iteration	Healthy	Bearing	Gear
1	-24.034	-23.566	-21.26
2	-23.246	-19.411	-21.683
3	-24.559	-23.93	-21.095

Signal intensity (dB) @ 2040 RPM			
Iteration	Healthy	Bearing	Gear
1	-9.5048	-4.1706	-7.0542
2	-8.4935	-5.0862	-7.2232
3	-8.3454	-5.7704	-5.2722

In summary, the audio sensor is able to detect both bearing fault and gear fault with good confidence level. At a fixed motor speed, one of the major vibration modes is able to detect the faulty condition of the equipment. When the motor speed is changing, the major vibration modes tend to change, which requires determining the right

vibration mode for the equipment fault detection.

3. Conclusions

Both magnetic sensor and audio sensor are able to detect the equipment fault without the contact mounting to the equipment. The magnetic sensor can detect the gear fault at different motor speeds with high confidence level. The audio sensor is able to detect both bearing fault and gear fault. However, the vibration mode has to be determined at different motor speed.

REFERENCES

1. Mubarak A., Barmak H. S. A., and Muhammad K., "Non-Invasive Inspections: A Review on Methods and Tools", Sensors 2021, 21, 8474.
2. Muhammad A., Tallha A., Muhammad A. K. , Muhammad I., Munawwar I., and Hsu C.-H., "A New Statistical Features Based Approach for Bearing Fault", Sensors 2022, 22, 2012.
3. Sun J., Yan C., and Wen J., "Intelligent Bearing Fault Diagnosis Method Combining Compressed Data Acquisition and Deep Learning", IEEE Trans. Instrum. Meas., Vol. 67, No. 1, pp.185-195, 2018.